ACS Macro Letters

Letter

pubs.acs.org/macroletters

Janus Polymer Single Crystal Nanosheet via Evaporative Crystallization

Hao Qi, Wenda Wang, and Christopher Y. Li*

Department of Materials Science and Engineering, Drexel University, Philadelphia, Pennsylvania 19104, United States

Supporting Information

ABSTRACT: We show that liquid/liquid interface can guide polymer chain folding during crystallization. Evaporation-induced crystallization of telechelic dicarboxyl end-functionalized poly(ε-caprolactone) (COOH-PCL-COOH) at a water/pentyl acetate interface produced millimeter-scale, uniform polymer single crystal (PSC) films. Due to the asymmetric nature at the interface, the PSC nanosheets exhibited a Janus structure: the two surfaces of the crystal showed distinct water contact angle, which are quantitatively confirmed by in situ nanocondensation using environmental scanning electron microscopy (ESEM).

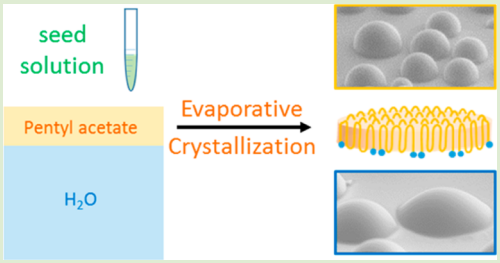

Janus particles with a noncentrosymmetric structure have attracted great attention during the past decade because of their unique properties associated with the broken symmetry of the particles.[1] According to their shapes, Janus nanostructures can be divided into zero-dimensional (0D) Janus nanospheres, one-dimensional (1D) Janus cylinders or nanowires, and two-dimensional (2D) Janus nanosheets. Both all-organic and hybrid Janus particles comprised of an inorganic/metallic core and an organic/polymeric shell have been reported.[1] While extensive work has been reported on hybrid Janus nanosphere and nanowires, reports on the preparation of 2D Janus nanosheet are limited. Gruning et al. showed that crushing hydrophobized hollow glass particles led to large quantity of Janus sheets.[2] Liang et al. achieved large-scale production of inorganic Janus nanosheets by crushing silica shells whose chemically distinct interior/exterior surfaces.[3] Stupp et al. reported the synthesis of 2D asymmetric polymer sheets.[4] Walther et al. demonstrated the preparation of Janus discs based on controlled phase separation of block terpolymer, where the Janus discs were obtained by selective cross-linking and partial dissembling of the self-assembled supramolecular structure.[5] Most recently, Deng et al. fabricated Janus nanodiscs by stepwise disassembling disc-stacked particles of polystyrene-*b*-poly(4-vinylpyridine).[6]

As the building block of polymer spherulites, polymer single crystals (PSC) are typically 2D lamellae with a thickness of several nanometers.[7] They can be formed in solution or thin films with several hundreds of nanometers to micrometers in lateral size. Morphologically, these PSC lamellae can be regarded as quasi-2D materials with controlled shape, size, and crystallinity. In addition, polymer crystallization is a bottom up self-assembly process involving polymer chains folding back and forth within the lamellae. With carefully controlled crystallization conditions, the chain ends can be precisely located at the lamellar surface, rendering much needed functionality for PSCs to be used as nanoscale materials.[7b,8] Previous work has demonstrated that these surface functionalized PSCs can be used to immobilize various nanoparticles,[9] enabling a plethora of functional materials for nanoparticle synthesis, surface enhanced Raman Spectroscopy, nanomotors, catalyst support, and so on.[9e,10] These PSCs are typically symmetric with the two lamellar surfaces bearing similar functional groups. It has been demonstrated asymmetric folding can occasionally lead to unbalanced lamellar surfaces.[11] Using ABC triblock copolymer with a crystalline B block, noncentrosymmetric polymer single crystals can form.[12] Polymer single crystals can also be formed in thin films, and the crystal morphology is critically dependent on the film thickness, substrate chemistry, and polymer chain ends.[13] At the air–water interface, polymer chains can also be assembled into a monolayer film by Langmuir–Blodgett technique. Crystallization of poly(ε-caprolactone) (PCL) and PCL-based copolymers at air–water interface has been reported.[14] Kumaki et al. observed isotactic poly(methyl methacrylate) crystallized into 2D folded-chain crystal of its Langmuir monolayer film upon compression.[15] With pinned nucleation agents at the liquid/liquid interface, orthogonal growth of polymer crystals can be achieved.[16]

In this work, we report breaking the centrosymmetry of a single crystal lamella using an evaporative crystallization process on water surface. Evaporation-driven nanoparticle assembly has been extensively studied.[17] Controlled solvent annealing has also been widely used to induce/improve polymer self-assembly. In the present work, we first create an oil/water interface where crystalline dicarboxyl end-functionalized PCL (COOH-PCL-COOH, M_n=7200, 2500 g/mol) is dissolved in the oil phase, evaporation of which induces PCL crystallization. Millimeter scale uniform PCL lamellae are formed with the carboxyl end groups pinned at the water surface, which breaks

Received: May 11, 2014
Accepted: June 24, 2014
Published: June 27, 2014

the centrosymmetry of the PCL lamella, leading to Janus PSC nanosheets. The Janus nature of the PSC sheet is confirmed by in situ water vapor nanocondensation using environmental scanning electron microscopy (ESEM).

Figure 1a shows the evaporative crystallization process of COOH-PCL-COOH at water/pentyl acetate interface. In the

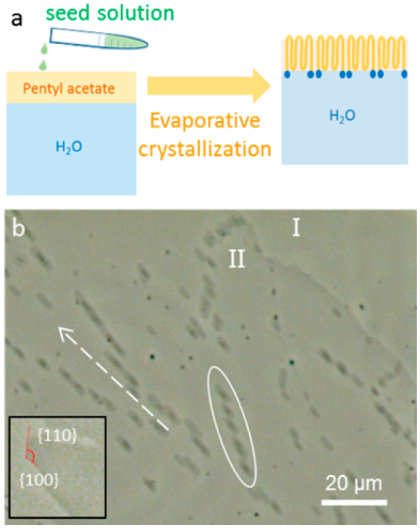

Figure 1. (a) Schematic illustration of the crystallization procedure of COOH-PCL-COOH nanosheet at the water/pentyl acetate interface; (b) phase-contrast microscopy image of the PCL nanosheet; inset shows {110} and {100} planes of PCL.

experiment, PCL/1-butanol solution with a concentration of 0.03 wt % was prepared at 60 °C and was subsequently cooled to −10 °C for 2 h. The solution was then brought to 44.5 °C for 10 min to produce polymer seeds. A total of 200 μL of the as-prepared polymer seed solution was drop-wisely transferred to a pentyl acetate/water biphasic solution with 1 g pentyl acetate covering the water surface, as shown in Figure 1a. The evaporative crystallization occurred at ambient temperature for approximately 4 days, when the organic solvent evaporated and a polymer film was formed. COOH-PCL-COOH can be seen as an amphiphile with its hydrophobic backbone and hydrophilic carboxyl end groups. Pentyl acetate is chosen as the organic phase because of its immiscibility with water and the lower density to float on the water surface. Moreover, our previous work showed that pentyl acetate induced PCL single crystal growth upon evaporation.[18] Upon crystallization, we envisage that COOH groups will be pinned at the water surface, and noncentrosymmetric PCL single crystals can be obtained (Figure 1a).

Figure 1b shows a phase-contrast optical microscopy image of the resultant quasi 2D PCL nanosheet. Part I in the image refers to the background; part II is the PSC sheet, and the inset shows the PCL single crystal with clear facets. The red line annotated angle is 125°, corresponding to the angle between {110} and {100} faces of PCL. The gray elongated rods on top of the PSC sheet appear to be overgrown PCL crystals, probably due to excess polymers added. Of interest is that all the long axes of the rods are parallel with each other. Based on PCL single crystal structure and morphology,[19] the long axis of the rods represents PCL crystal *b*-axis, and the uniform alignment of these *b*-axes suggest that, disregarding the fold surface of the PCL crystals, this overgrowth follows an epitaxial growth mechanism with the substrate and, more importantly, the underlying PSC nanosheet is a single crystal with a uniform crystal orientation.

The crystal structure of the PCL nanosheet can be confirmed using selected area electron diffraction (SAED) experiments, as shown in Figure 2a. The SAED pattern is consistent with the

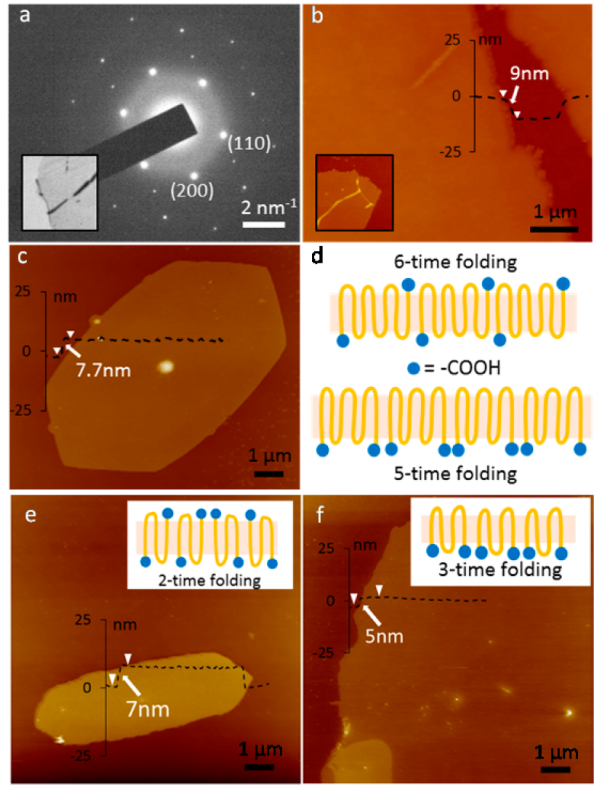

Figure 2. (a) Electron diffraction pattern of COOH-PCL-COOH single crystal film, inset: Transmission electron microscopy (TEM) image (horizontal field width = 11 μm); (b) Atomic force microscopy (AFM) images of COOH-PCL-COOH single crystal nanosheet and the corresponding height profile, inset: morphology of a PCL single crystal tip (horizontal field width = 2.5 μm); (c) AFM image of COOH-PCL-COOH single crystal prepared through solution crystallization and the corresponding height profile; (d) Side views of COOH-PCL-COOH crystals showing the chain folding during solution crystallization (top) and evaporative crystallization (bottom). (a–d) represent PCL with a 7200 g/mol molecular weight. (e and f) AFM images of COOH-PCL-COOH (M_n = 2.5 K g/mol) prepared from solution crystallization (e) and evaporative crystallization (f). Insets show side view of corresponding chain folding.

reported PCL orthorhombic unit cell, a = 0.748, b = 0.498, and c = 1.726 nm.[20] Only (hk0) diffraction planes are observed, indicating that the *c*-axis and the polymer chain is perpendicular to the PSC nanosheet. The overall thickness of the PSC sheet is measured to be about 9 nm using atomic force microscopy (AFM, Figure 2b). Considering the PCL unit cell parameters and the molecular weight of PCL, we can conclude that a single COOH-PCL-COOH chain folds 5 times along the direction perpendicular to the film surface (Figure 2d). In comparison, our control experiment shows that the COOH-PCL-COOH PSC crystallized in solution under the same condition is 7.7 nm thick, which corresponds to 6-time folding. As shown in Figure 2d, 6-time folding of the PCL chain leads to a symmetric lamella, which the chain ends evenly distributed on both

dx.doi.org/10.1021/mz5002806 | *ACS Macro Lett.* 2014, 3, 675–678

surfaces of the lamella. At the water/pentyl acetate interface, all carboxyl groups are pinned at the water surface during crystallization, and such a chain conformation is incommensurate with 6-time folding. Consequently, 5-time folding was formed in the evaporative crystallization case where the lamellar thickness increased from 7.7 to 9 nm. We further used 2.5 K g/mol COOH-PCL-COOH to conduct similar experiments. As shown in Figure 2e,f, the polymer chains fold two and three times when crystallize in solution, or at the interface, respectively. This is consistent with our results using 7.2 K g/mol PCL.

It has been a challenging task to confirm the Janus nature of nanoparticles, particularly when the length scale is sub-20 nm.[1a] Typically, staining is used for microscopy experiments, while contrast has been an issue in many cases.[1a] In the present work, we validated the Janus property of our PSC nanosheets by measuring water contact angles on each side using in situ water condensation under ESEM. In situ condensation, instead of sessile drop, was used to better reveal the local wettability information with small water droplets (40−100 μm in diameter).[21] Detailed experimental condition and data analysis can be found in Supporting Information. In brief, a sample was mounted to a 60° tilted stage, as shown in Figure S1. The Peltier cooler stage on the back of the sample was kept at 1 °C and the initial vapor pressure was 3 Torr. To induce water condensation, the vapor pressure was slowly increased at the rate of 0.1 Torr per 20 s, until a condensation droplet is observed. Afterward, the vapor pressure was kept constant and the droplets can be considered as in an equilibrium state (negligible growth when the images were captured). Figure 3

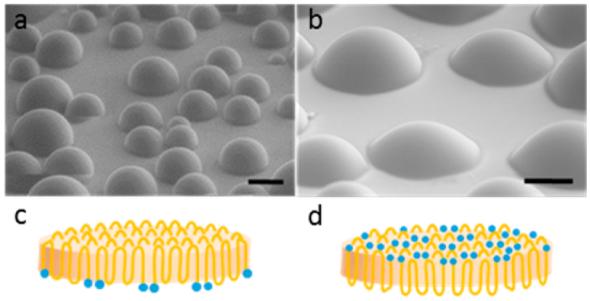

Figure 3. ESEM image of water droplets condensed on (a) hydrophobic side; (b) hydrophilic side of the PSC (7.2 K g/mol) nanosheet. Scale bar is 25 μm. (c, d) Schematic showing of the corresponding surface composition. Top surfaces are in contact with water droplets.

shows the ESEM image of water droplets condensed on the PSC (M_n = 7.2 K g/mol) nanosheet surface that was facing the pentyl acetate (a) and water (b) phase during crystallization; and the calculated contact angles are 82 ± 1° (a) and 61 ± 5° (b), respectively (for detailed calculation, see Supporting Information). It is therefore evident that the contact angle of the two sides of the PSC nanosheets directly exhibits hydrophobicity difference. Meanwhile, the vapor pressure required to condense for both sides is different: 5.3 Torr for the more hydrophobic side versus 4.9 Torr for the more hydrophilic side, implying a higher energy barrier for water vapor to condense on the hydrophobic side. Thus, both the contact angle and vapor pressure measurements suggest the PSC film obtained from the evaporative crystallization is a Janus nanosheet.

The above observed water contact angles can be quantitatively reconciled with PCL nanosheet surface chemistry using the concept of composite contact angle. The apparent contact angle of a composite surface θ', as proposed by Cassie in 1948, can be described as[22]

$$\cos\theta' = f_1 \cos\theta_1 + f_2 \cos\theta_2 \quad (1)$$

where f_1 and f_2 are the surface area fractions of two different surface components with the corresponding contact angles of θ_1 and θ_2, respectively. $f_1 + f_2 = 1$. Assuming that the only difference between the two sides of the PSC nanosheets is the concentration of carboxyl groups, we can divide the PSC surface chemistry groups into two types, the caprolactone and carboxyl groups.[23] We adopt 81° and 10° as their intrinsic contact angles.[23] Based on the above equation, the relationship between composite contact angle and carboxyl group surface areal density is plotted in Figure 4, which shows that the

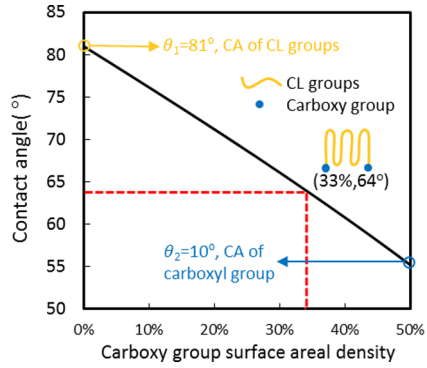

Figure 4. Plot of CL−carboxyl composites surface contact angle as a function of the carboxyl group surface areal density. Inset: schematic illustration of the side view of a PSC film showing 5-time chain folding.

apparent contact angle of a PCL−carboxyl composites surface decreases with increasing carboxyl group areal density. From this plot, the contact angle of the PSC film's hydrophilic side can be estimated: A 5-time folded polymer chain yields 6 stems where 2 of them are carboxyl group, resulting in approximately 33% carboxyl group surface areal density, if we assume these two groups occupy similar surface areas. Correspondingly, the calculated contact angle is 64°, which is very close to our ESEM condensation result, and confirms our hypothesis that carboxyl end groups are all pinned at the water surface. Therefore, liquid−liquid interface is demonstrated to be an efficient strategy to guide polymer chain folding during crystallization.

In summary, we have fabricated Janus polymer single crystals using evaporative crystallization at water/pentyl acetate interface. Telechelic COOH-PCL-COOH crystallizes at water/pentyl acetate interface upon evaporation of pentyl acetate. Water phase pinned the hydrophilic chain ends, altered chain folding conformation, and led to a noncentrosymmetric Janus single crystal nanosheet. In situ nanocondensation experiments quantitatively demonstrated the Janus nature of the nanosheets. We anticipate that our approach can be used to fabricate ordered Janus 2D materials with various sizes and functions.

■ ASSOCIATED CONTENT

Supporting Information

Detailed experimental procedures and tomography reconstructed movie. This material is available free of charge via the Internet at http://pubs.acs.org.

dx.doi.org/10.1021/mz5002806 | ACS Macro Lett. 2014, 3, 675−678

AUTHOR INFORMATION

Corresponding Author

*E-mail: chrisli@drexel.edu.

Notes

The authors declare no competing financial interest.

ACKNOWLEDGMENTS

This work was supported by the National Science Foundation Grant DMR-1308958.

REFERENCES

(1) (a) Walther, A.; Müller, A. H. *Chem. Rev.* **2013**, *113*, 5194−5261. (b) Jiang, S.; Chen, Q.; Tripathy, M.; Luijten, E.; Schweizer, K. S.; Granick, S. *Adv. Mater.* **2010**, *22*, 1060−1071. (c) De Gennes, P. G. *Rev. Mod. Phys.* **1992**, *64*, 645−648. (d) Lee, K. J.; Yoon, J.; Lahann, J. *Curr. Opin. Colloid Interface Sci.* **2011**, *16*, 195−202. (e) Glotzer, S. C.; Solomon, M. J. *Nat. Mater.* **2007**, *6*, 557−562.

(2) Gruning, B.; Holtschmidt, V.; Koerner, G.; Rossmy, G. U.S. Patent 4,715,19, July 4,1989.

(3) Liang, F.; Shen, K.; Qu, X.; Zhang, C.; Wang, Q.; Li, J.; Liu, J.; Yang, Z. *Angew. Chem., Int. Ed.* **2011**, *50*, 2379−2382.

(4) Stupp, S. I.; Son, S.; Lin, H. C.; Li, L. S. *Science* **1993**, *259*, 59−63.

(5) (a) Walther, A.; André, X.; Drechsler, M.; Abetz, V.; Müller, A. H. E. *J. Am. Chem. Soc.* **2007**, *129*, 6187−6198. (b) Walther, A.; Göldel, A.; Müller, A. H. E. *Polymer* **2008**, *49*, 3217−3227. (c) Wolf, A.; Walther, A.; Müller, A. H. E. *Macromolecules* **2011**, *44*, 9221−9229.

(6) Deng, R.; Liang, F. X.; Zhou, P.; Zhang, C. L.; Qu, X. Z.; Wang, Q.; Li, J. L.; Zhu, J. T.; Yang, Z. Z. *Adv. Mater.* **2014**, DOI: 10.1002/adma.201305849.

(7) (a) Geil, P. *Polymer Single Crystals*; Robert Krieger Pub.: Huntington, N.Y., 1973. (b) Li, C. Y. *J. Polym. Sci., Part B: Polym. Phys.* **2009**, *47*, 2436−2440.

(8) Laird, E. D.; Li, C. Y. *Macromolecules* **2013**, *46*, 2877−2891.

(9) (a) Wang, B. B.; Li, B.; Ferrier, R. C. M.; Li, C. Y. *Macromol. Rapid Commun.* **2010**, *31*, 169−175. (b) Wang, B. B.; Li, B.; Dong, B.; Zhao, B.; Li, C. Y. *Macromolecules* **2010**, *43*, 9234−9238. (c) Wang, B. B.; Dong, B.; Li, B.; Zhao, B.; Li, C. Y. *Polymer* **2010**, *51*, 4814−4822. (d) Li, B.; Wang, B. B.; Ferrier, R. C. M.; Li, C. Y. *Macromolecules* **2009**, *42*, 9394−9399. (e) Wang, B. B.; Li, B.; Zhao, B.; Li, C. Y. *J. Am. Chem. Soc.* **2008**, *130*, 11594−11595. (f) Li, B.; Ni, C.; Li, C. Y. *Macromolecules* **2008**, *41*, 149−155. (g) Li, B.; Li, C. Y. *J. Am. Chem. Soc.* **2007**, *129*, 12−13.

(10) (a) Zhou, T.; Wang, B.; Dong, B.; Li, C. Y. *Macromolecules* **2012**, *45*, 8780−8789. (b) Zhang, H.; Dong, B.; Zhou, T.; Li, C. Y. *Nanoscale* **2012**, *4*, 7641−7645. (c) Dong, B.; Li, B.; Li, C. Y. *J. Mater. Chem.* **2011**, *21*, 13155−13158. (d) Dong, B.; Wang, W.; Miller, D. L.; Li, C. Y. *J. Mater. Chem.* **2012**, *22*, 15526−15529. (e) Dong, B.; Zhou, T.; Zhang, H.; Li, C. Y. *ACS Nano* **2013**, *7*, 5192−5198. (f) Dong, B.; Miller, D. L.; Li, C. Y. *J. Phys. Chem. Lett.* **2012**, *3*, 1346−1350. (g) Zhou, T.; Dong, B.; Qi, H.; Lau, H. K.; Li, C. Y. *Nanoscale* **2014**, *6*, 4551−4554.

(11) (a) Lotz, B.; Cheng, S. Z. D. *Polymer* **2005**, *46*, 577−610. (b) Cai, W.; Li, C. Y.; Li, L.; Lotz, B.; Keating, M.; Marks, D. *Adv. Mater.* **2004**, *16*, 600−605.

(12) Xiong, H.; Chen, C.-K.; Lee, K.; Van Horn, R. M.; Liu, Z.; Ren, B.; Quirk, R. P.; Thomas, E. L.; Lotz, B.; Ho, R.-M.; Zhang, W.-B.; Cheng, S. Z. D. *Macromolecules* **2011**, *44*, 7758−7766.

(13) (a) Zhang, G.; Cao, Y.; Jin, L.; Zheng, P.; Van Horn, R. M.; Lotz, B.; Cheng, S. Z. D.; Wang, W. *Polymer* **2011**, *52*, 1133−1140. (b) Zhang, G.; Zhai, X.; Ma, Z.; Jin, L.; Zheng, P.; Wang, W.; Cheng, S. Z. D.; Lotz, B. *ACS Macro Lett.* **2012**, *1*, 217−221. (c) Chen, E. Q.; Jing, A. J.; Weng, X.; Huang, P.; Lee, S. W.; Cheng, S. Z. D.; Hsiao, B. S.; Yeh, F. J. *Polymer* **2003**, *44*, 6051−6058. (d) Zhu, D.-S.; Liu, Y.-X.; Chen, E.-Q.; Li, M.; Chen, C.; Sun, Y.-H.; Shi, A.-C.; Van Horn, R. M.; Cheng, S. Z. D. *Macromolecules* **2007**, *40*, 1570−1578.

(14) (a) Joncheray, T. J.; Denoncourt, K. M.; Mathieu, C.; Meier, M. A. R.; Schubert, U. S.; Duran, R. S. *Langmuir* **2006**, *22*, 9264−9271. (b) Li, B.; Esker, A. R. *Langmuir* **2007**, *23*, 2546−2554. (c) Li, B.; Wu, Y.; Liu, M.; Esker, A. R. *Langmuir* **2006**, *22*, 4902−4905.

(15) (a) Kumaki, J.; Kawauchi, T.; Yashima, E. *J. Am. Chem. Soc.* **2005**, *127*, 5788−5789. (b) Takanashi, Y.; Kumaki, J. *J. Phys. Chem. B* **2013**, *117*, 5594−5605.

(16) Wang, W.; Li, C. Y. *ACS Macro Lett.* **2014**, *3*, 175−179.

(17) Han, W.; Lin, Z. *Angew. Chem., Int. Ed.* **2012**, *51*, 1534−1546.

(18) (a) Chen, X.; Wang, W.; Cheng, S.; Dong, B.; Li, C. Y. *ACS Nano* **2013**, *7*, 8251−8257. (b) Chen, X.; Dong, B.; Wang, B. B.; Shah, R.; Li, C. Y. *Macromolecules* **2010**, *43*, 9918−9927.

(19) Núñez, E.; Gedde, U. W. *Polymer* **2005**, *46*, 5992−6000.

(20) Hu, H.; Dorset, D. L. *Macromolecules* **1990**, *23*, 4604−4607.

(21) (a) Brugnara, M.; Volpe, C. D.; Siboni, S.; Zeni, D. *Scanning* **2006**, *28*, 267−273. (b) Jung, Y. C.; Bhushan, B. *J. Microscopy* **2008**, *229*, 129−140.

(22) Cassie, A. *Trans. Faraday Soc.* **1944**, *40*, 456.

(23) Cecchet, F.; Pilling, M.; Hevesi, L.; Schergna, S.; Wong, J. K. Y.; Clarkson, G. J.; Leigh, D. A.; Rudolf, P. *J. Phys. Chem. B* **2003**, *107*, 10863−10872.